Supporting Information for

Mössbauer, EPR, and DFT Studies of Synthetic S = ½ Fe^{III}-O-Fe^{IV}=O Complexes: Superexchange-Mediated Spin Transition at the Fe^{IV}=O Site

Raymond F. De Hont[†], Genqiang Xue[‡], Michael P. Hendrich[†], Lawrence Que, Jr. [‡], Emile L. Bominaar[†], Eckard Münck[†]

Contribution from the Department of Chemistry, Carnegie Mellon University, Pittsburgh, Pennsylvania, 15213 and Department of Chemistry and Center for Metals in Biocatalysis, University of Minnesota, 207 Pleasant Street SE, Minneapolis, MN 55455

EPR Temperature Dependence of 1-OH

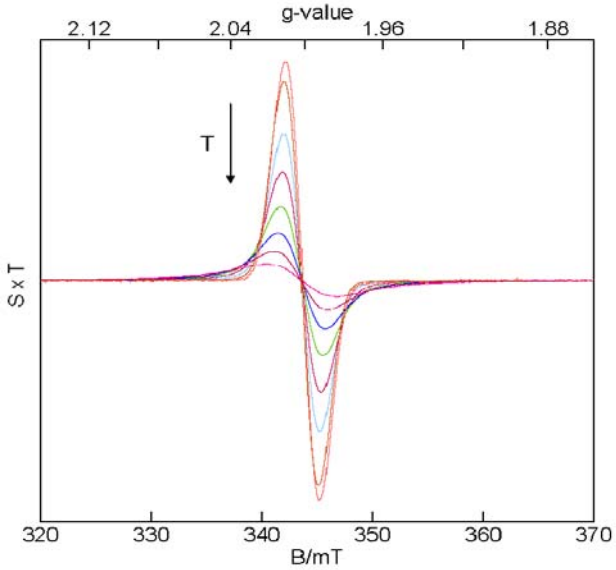

Figure S1. X-band (9.63 GHz) EPR spectra of **1-OH** in 3:1 CH_2Cl_2/MeCN at temperatures 27 K → 140 K plotted as signal × T. Experimental conditions are the same as those in Figure 3.

Determination of Exchange Coupling Constant by EPR for 1-F

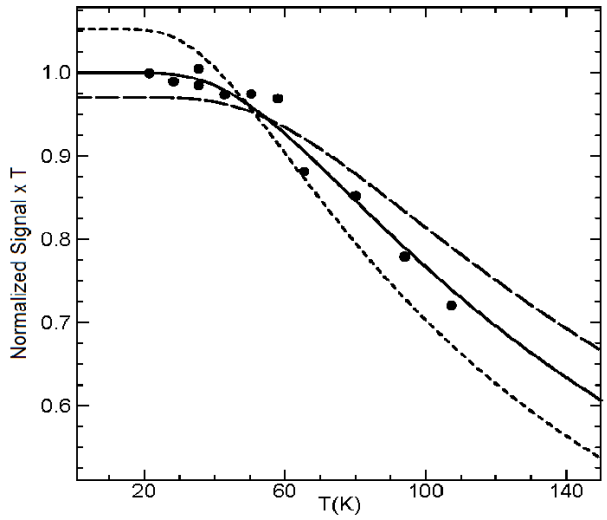

Figure S2. Temperature dependence of the population of the S = ½ ground state of **1-F**. The solid line is a fit for 90 cm^{-1}. The dashed curves were calculated for J = 70 and 110 cm^{-1}.

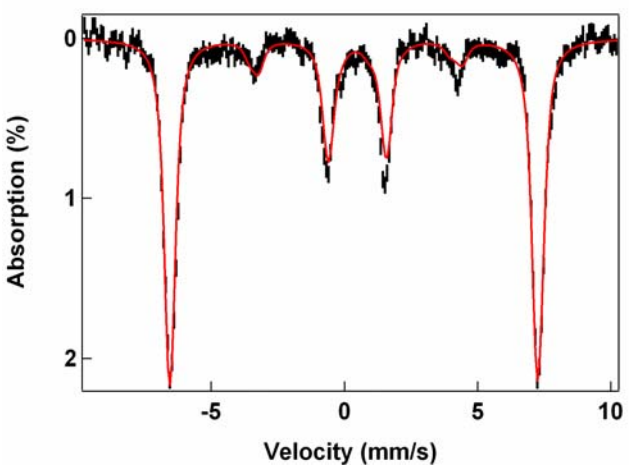

Figure S3. Mössbauer spectrum of $[Fe^{III}(L)Cl_2]^+$ in butyronitrile recorded at 4.2 K in a field of 8 T applied parallel to the observed γ-radiation. The red line, accounting for approximately 90% of the Fe, is a spectral simulation for the following S = 5/2 parameter set: D = 1 cm^{-1}; E/D = 0.2; $A_{iso}/g_n\beta_n$ = –20.4 T; δ = 0.43 mm/s; ΔE_Q = 0.43 mm/s and η = 1.0.

DFT Results for 1-F_m

The computational model **1-F_m** has the same spin state as **1-OH_m**, namely S = 1/2. The J-value calculated for the couple (S_a = 5/2, S_b = 2) in **1-F_m**, J = +104 cm^{-1}, is in good agreement with the experimental value, J = 90 ± 20 cm^{-1}, and somewhat smaller than in **1-OH_m**. The scheme of Figure S4 shows that the (5/2, 2) 9/2 level is now slightly above, ca. 120 cm^{-1}, the (5/2, 1) 3/2 level (Table S2). The J for the couple (5/2, 1) is ferromagnetic and places the (5/2, 1) 7/2 level between the (5/2, 1) 3/2 and (5/2, 2) 1/2 levels. Unlike in **1-OH_m**, where (5/2, 1) 7/2 is the upper level, (5/2, 2) 9/2 is the highest level in **1-F_m** (Figure S4). However, this change does not affect the ground state, which is (5/2, 2) 1/2 in both **1-F_m** and **1-OH_m** due to the strong antiferromagnetic exchange in the (5/2, 2) couples of these systems.

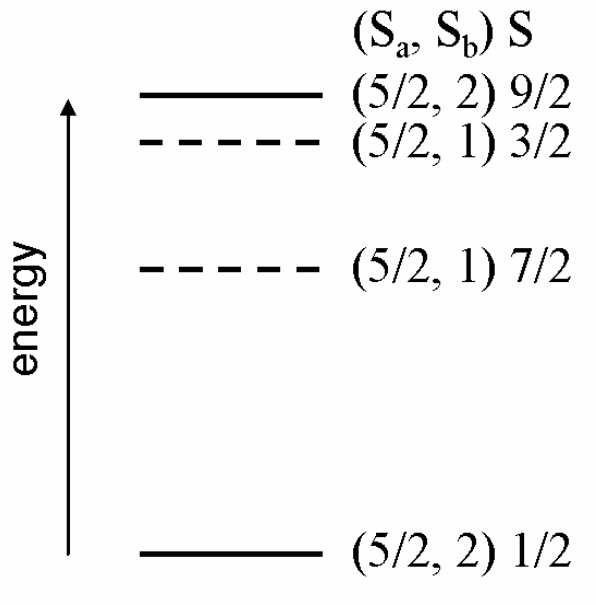

Figure S4. Energy level scheme for **1-F$_m$** obtained with DFT, *cf*. Table S1. Shown are the top and bottom levels of the (5/2, 2) and (5/2, 1) spin ladders. The (5/2, 1) pair is ferromagnetically coupled.

In section 4.3 we showed for **1-OH$_m$** that the energy gap between (5/2, 1) 7/2 and (5/2, 2) 1/2 can be decomposed into a large antiferromagnetic exchange contribution and a smaller ligand-field change contribution, the latter being approximately equal to the gap between (5/2, 1) 7/2 and (5/2, 2) 9/2 (see Figure 13). Comparison of Figure S4 and Figure 13 shows that the (5/2, 1) 7/2 and (5/2, 2) 9/2 levels in **1-F$_m$** appear in reversed order compared to those in **1-OH$_m$**. Although we do not yet fully understand the difference between **1-OH$_m$** and **1-F$_m$**, the following considerations may shed light on its origin. A number of contributions to J have been described in the literature.[1] These include those arising from interactions of the ground configuration with metal-to-metal charge transfer configurations and from exchange interactions between the unpaired electrons in the ground configuration. As the latter couplings are often small, we focus on the CT contributions. The CT mechanism gives for exchange channels with singly occupied d-orbitals, (d_a^1, d_b^1), antiferromagnetic contributions to J, whereas CT in (d_a^1, d_b^0) and (d_a^1, d_b^2) channels gives ferromagnetic contributions.[2] In the case that only the antiferromagnetic (d_a^1, d_b^1) mechanism is operative, the energies for the ferromagnetic states, (5/2, 1) 7/2 and (5/2, 2) 9/2, are unaffected while states with lower values for the

total spin are increasingly lowered in energy as a function of decreasing value of S, leading to states with spins 3/2 and 1/2 at the bottom of the spin ladders for the (5/2, 1) and (5/2, 2) couples, respectively. The relative energies of top levels, (5/2, 1) 7/2 and (5/2, 2) 9/2, are then determined by local interactions, such as the ligand field, as described in section 4.3. This is the situation found in **1-OH$_m$**. The ferromagnetic exchange coupling for the (5/2, 1) couple in **1-F$_m$** suggests that the ferromagnetic contributions to J from CT in (d_a^1, d_b^0) and (d_a^1, d_b^2) contribute as well in this system, such that both the (5/2, 1) 7/2 and (5/2, 1) 3/2 states are stabilized and positioned below the (5/2, 2) 9/2 state (Figure S4). The difference in the exchange coupling of the (5/2, 1) couples in **1-OH$_m$** and **1-F$_m$** may be rooted in the different bridging geometry of the oxo bridges in the two systems (bent in the **1-OH** and linear in **1-F**). **1-F$_m$** and **1-OH$_m$** have in common a strong antiferromagnetic exchange in the (5/2, 2) couple. The antiferromagnetic interaction lowers the energy of (5/2, 2) 1/2 while leaving the energy of (5/2, 2) 9/2 unchanged (see above), resulting in a (5/2, 2) 1/2 ground state for **1-F$_m$** (Figure S4) in which $S_b = 2$.

Table S1. DFT results for **1-F$_m$** and **1-OH$_m$**[a]

($S[Fe_F^{III}]$,$S[Fe_O^{IV}]$)S	ΔE (cm^{-1})	J (cm^{-1})	Fe_F^{III}–O_B (Å)	Fe_O^{IV}–O_B (Å)	Fe–O_B–Fe (°)	Fe_F^{III}–F (Å)
			1-F$_m$			
(5/2, 2) 1/2	0	+104	1.800	1.811	175	1.914
(5/2, 2) 9/2	1248		1.808	1.837	175	1.916
(5/2, 1) 3/2	1129	−59	1.787	1.858	173	1.934
(5/2, 1) 7/2	775		1.786	1.862	172	1.933
			1-OH$_m$			
(5/2, 2) 1/2	0	+135	1.887	1.807	129	1.859
(5/2, 2) 9/2	1620		1.907	1.827	129	1.864
(5/2, 1) 3/2	1709	+69	1.861	1.873	129	1.870
(5/2, 1) 7/2	2123		1.858	1.879	131	1.876

[a] The results for **1-OH$_m$** are the same as in Table 4 and have been added to facilitate the comparison of the two species.

Let us now consider the structural data in Table S1. The ligand change between **1-OH$_m$** and **1-F$_m$** has an important effect on the structure. The O= Fe_O^{IV} –O_B– Fe_F^{III} –F unit is planar with a dihedral angle of 180° (Figure 12) and the Fe–O_B–Fe bridge is nearly linear (Table

S1). The distances in the core units of **1-OH$_m$** and **1-F$_m$** are compared in the following scheme:

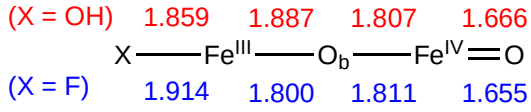

This comparison shows that the Fe^{IV} half is relatively unaffected by the nature of X but that the Fe^{III} half is quite sensitive. Indeed the Fe^{III}–O_B changes seem to be dictated by the strength of the Fe–X interaction. The Fe^{III}–O_B bond in **1-F$_m$** is ~0.08 Å shorter than in **1-OH$_m$**, and correlates with an Fe^{III}_{F}–F distance that is 0.06 Å longer than the Fe^{III}_{OH}–O_H distance. Fe^{III}–O_H is shorter than Fe^{III}–F possibly because the hydrogen bonding in **1-OH$_m$** makes the O_H more basic than F. This engenders a lengthening of the Fe^{III}–O_B bond in **1-OH$_m$**. The Fe^{IV}–O_B distances in both complexes are virtually identical. Despite the large difference in Fe^{III}–O_B bond length between **1-OH$_m$** and **1-F$_m$**, the spin description remains by and large the same and so does the J value.

For any given spin couple (S_a, S_b) listed in Tables 4 and S1, the average of the two Fe–O_B bond distances (denoted P) is shortest for the coupled spin state (S) with the lowest energy. For example, in **1-OH$_m$** P = 1.847 Å for ground state (5/2, 2) 1/2 and P = 1.867 Å for excited state (5/2, 2) 9/2 (Table 4), corresponding to a shortening of 0.02 Å in the lowest state. The shortening is an example of spin-dependent structural relaxation by which a system is lowering the energy of the lowest state in the exchange ladder by enhancing the exchange-coupling constant. This change is also found for **1-F**.

There are also complementary changes in the two bridging Fe–O bond distances in **1-OH$_m$** and **1-F$_m$** in their response to local spin states. In the transition $S[Fe^{IV}_{O}] = 1 \rightarrow 2$, the Fe^{IV}–O_B bond shortens by 0.05 Å (**1-OH$_m$**) and 0.04 Å (**1-F$_m$**), while the Fe^{III}–O_B bond lengthens by 0.03 Å (**1-OH$_m$**) and 0.02 Å (**1-F$_m$**) (Tables 4 and S1).

Relation between $E(S_b = 1) - E(S_b = 2)$ and Fe_O^{IV} –O_B bond length

The stabilization of the high-spin state of a metal center by shortening of the bond length to one of its ligands (Section 4.3) seems counterintuitive and asks for an explanation. As discussed in Section 4.3, the $S[Fe_O^{IV}] = 1 \rightarrow 2$ transition involves the excitation $xy^{\beta} \rightarrow (x^2\text{-}y^2)^{\alpha}$ (see Figure 12 for axes convention). Thus, the shortening of the Fe^{IV}–O_B bond is expected to affect the transition energy in two antagonistic ways: the antibonding d_{xy} and $d_{x^2-y^2}$ orbitals are both raised in energy, respectively decreasing and increasing the excitation energy. The net reduction of the $d_{x^2-y^2} - d_{xy}$ energy gap points toward the prevalence of the change in the d_{xy} energy. The d_{xy} orbital is more susceptible than $d_{x^2-y^2}$ to the Fe^{IV}–O_B bond length because of its strong π interaction with the p_y orbital of O_B.

Spin Populations of 1-OH_m and 1-F_m

The spin populations of the iron centers in complexes **1-OH_m** and **1-F_m**, given in Table S2, are smaller in magnitude than the unpaired electron numbers 5, 4, and 2 for Fe^{III} (S = 5/2), Fe^{IV} (S = 2) and Fe^{IV} (S = 1), respectively. The differences are due to delocalization of unpaired spin density onto the ligands. The spin populations in Table S2 closely resemble the spin populations (4.2) calculated for the S = 5/2 state of the mononuclear complex $[(HO)_2Fe^{III}(L)]^{1+}$ and the spin populations (3.2 and 1.4) calculated for the S = 2 and S = 1 states, respectively, of the mononuclear complex $[(HO)(O)Fe^{IV}(L)]^{1+}$. The negative spin populations in Table S2 reflect the broken-symmetry character of the electronic configurations that represent the antiferromagnetic states (S = 1/2 and 3/2) in the first column of the table. Thus, the iron sites in the binuclear complexes **1-OH_m** and **1-F_m** closely resemble those in mononuclear compounds with similar ligands and show no sign of valence delocalization.

Table S2. Mulliken spin populations of DFT solutions for various spin states of **1-OH$_m$** and **1-F$_m$**.

$(S[Fe^{III}_X], S[Fe^{IV}_O])S$	X = OH^-		X = F^-	
	Fe^{III}	Fe^{IV}	Fe^{III}	Fe^{IV}
(5/2, 2) 1/2	4.2	–3.2	4.2	–3.2
(5/2, 2) 9/2	4.2	3.3	4.2	3.3
(5/2, 1) 3/2	4.2	–1.4	4.2	–1.3
(5/2, 1) 7/2	4.2	1.5	4.1	1.4

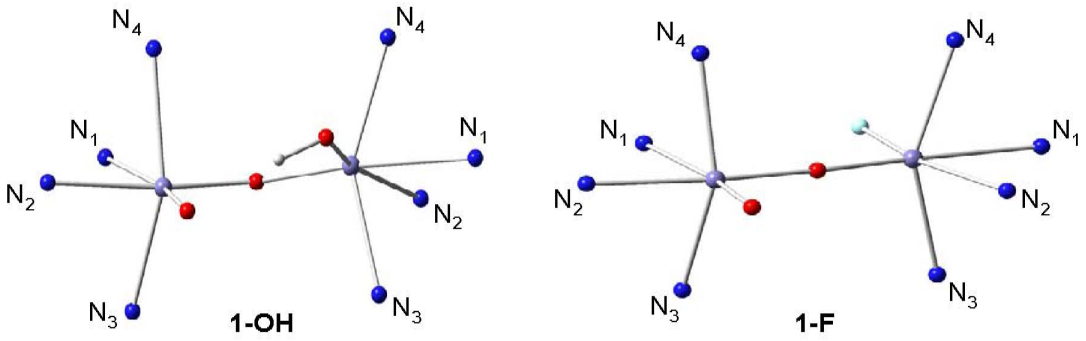

Figure S5. DFT-optimized structures of **1-OH$_m$** and **1-F$_m$** using labeling scheme of Table 2. Hydrogens and carbons have been omitted for clarity.

Table S3. DFT-calculated ^{14}N-hyperfine A-tensor components for **1-OH** and **1-F**.

		1-OH			**1-F**		
	Atom	A_x (MHz)	A_y (MHz)	A_z (MHz)	A_x (MHz)	A_y (MHz)	A_z (MHz)
Fe^{III}	**N_1 (amine)**	14	7	7	14	7	7
	N_2 (pyr.)	12	12	18	15	16	23
	N_3 (pyr.)	18	26	18	16	24	17
	N_4 (pyr.)	16	23	16	16	24	17
Fe^{IV}	**N_1 (amine)**	0	0	-2[a]	0	0	-1
	N_2 (pyr.)	-5	-3	-3	-6	-3	-3
	N_3 (pyr.)	-14	-19	-14	-14	-19	-14
	N_4 (pyr.)	-15	-20	-14	-14	-19	-14

[a] ^{14}N A-values have opposing signs at the Fe^{IV} and Fe^{III} sites, as expected for an antiferromagnetically coupled system.

Table S4. Cartesian coordinates (Å) for the broken symmetry (antiferromagnetic) (S = 1/2) DFT energy minimized model of **1-F$_m$**.

Atom	x	y	z	Atom	x	y	z
Fe	1.662494	-0.000105	-0.393049	H	5.082153	1.464419	-1.994674
Fe	-1.802912	0.000487	0.606677	H	3.519124	1.061454	-2.725668
O	-0.041234	-0.000136	0.186387	H	4.778646	-3.922915	-1.659502
O	-1.677225	0.000769	2.257258	H	4.779707	3.922274	-1.658099
N	3.888651	-0.000318	-0.962484	H	3.509669	-5.747606	-0.532251
C	4.032249	-1.242682	-1.782316	H	3.511162	5.746930	-0.530310
C	4.032587	1.242294	-1.781884	H	1.390064	-5.187074	0.673219
C	3.363778	-2.406908	-1.093857	H	1.391326	5.186573	0.674837
C	3.364388	2.406462	-1.093061	H	0.621007	-2.796981	0.693671
C	3.855019	-3.711031	-1.140541	H	0.621614	2.796689	0.694433
C	3.855989	3.710466	-1.139268	H	5.405935	-0.873443	0.241231
C	3.142029	-4.731924	-0.507669	H	5.406217	0.871944	0.241494
C	3.143240	4.731341	-0.506095	H	5.742072	-0.001203	2.819715
C	1.957477	-4.422484	0.164942	H	4.441196	-0.001263	4.938938
C	1.958561	4.422000	0.166335	H	1.938416	-0.000780	4.832667
C	1.520542	-3.101550	0.182612	H	0.833208	-0.000283	2.577872
C	1.521264	3.101180	0.183532	H	-2.070036	1.435449	-3.107799
N	2.209168	2.117065	-0.439287	H	-0.640955	1.066089	-2.139324
N	2.208680	-2.117414	-0.439916	H	-2.070705	-1.435149	-3.107509
C	4.749061	-0.000647	0.264475	H	-0.641457	-1.066190	-2.139123
C	3.982617	-0.000716	1.577533	H	-2.180804	3.931907	-2.708971
C	4.661131	-0.001007	2.799205	H	-2.182539	-3.931444	-2.708286
C	3.930028	-0.001038	3.986918	H	-2.595366	5.757681	-1.065077
C	2.532686	-0.000773	3.931709	H	-2.597520	-5.756848	-1.064088
C	1.908837	-0.000496	2.690105	H	-2.661497	5.209745	1.375911
N	2.630092	-0.000472	1.536771	H	-2.663038	-5.208567	1.376841
N	-2.346853	0.000365	-1.531574	H	-2.305274	2.819856	2.075532
C	-1.716186	1.245495	-2.090906	H	-2.305903	-2.818712	2.076081
C	-1.716756	-1.245150	-2.090658	H	-4.128712	0.874597	-2.305843
C	-2.011984	2.418971	-1.188296	H	-4.129109	-0.872214	-2.306987
C	-2.012958	-2.418362	-1.187837	H	-6.570040	-0.000648	-1.330700
C	-2.204629	3.722051	-1.649214	H	-7.764039	-0.000970	0.852530
C	-2.206139	-3.721434	-1.648554	H	-6.426953	-0.000264	2.970499
C	-2.436049	4.744523	-0.724740	H	-3.907784	0.000581	2.793341
C	-2.437786	-4.743702	-0.723910	F	1.344990	0.000185	-2.280842
C	-2.473854	4.442755	0.639716				
C	-2.475257	-4.441740	0.640510				
C	-2.281003	3.122727	1.039533				
C	-2.281891	-3.121719	1.040115				
N	-2.054846	-2.137785	0.140804				
N	-2.054151	2.138594	0.140383				
C	-3.844338	0.000740	-1.716251				
C	-4.619779	0.000188	-0.419999				
C	-6.016377	-0.000374	-0.402353				
C	-6.684018	-0.000547	0.822356				
C	-5.940902	-0.000164	2.006938				
C	-4.554135	0.000328	1.928971				
N	-3.912362	0.000490	0.734181				
H	5.081751	-1.464999	-1.995223				
H	3.518792	-1.061390	-2.726017				

Table S5. Cartesian coordinates (Å) for the broken symmetry (antiferromagnetic) (S = 1/2) DFT energy minimized model of **1-OH$_m$**.

Atom	x	y	z	Atom	x	y	z
Fe	-1.625117	0.080232	-0.448927	H	-3.246984	1.616813	-2.564441
Fe	1.707846	-0.099159	-0.311116	H	-4.783737	-1.082138	-2.721540
O	0.047257	-0.115845	0.401924	H	-3.192349	-0.413466	-3.142510
O	1.319241	-0.442160	-1.894042	H	-4.886007	4.046776	-1.026408
N	-3.813023	0.122279	-1.227297	H	-4.297830	-3.510395	-3.039907
C	-3.923393	1.530878	-1.713577	H	-3.937089	5.561210	0.709771
C	-3.779447	-0.867250	-2.344448	H	-2.945602	-5.494711	-2.373539
C	-3.452152	2.490558	-0.649465	H	-1.969922	4.788563	2.049136
C	-3.076888	-2.135265	-1.926345	H	-0.970788	-5.169197	-0.873128
C	-4.031792	3.742407	-0.439015	H	-1.028832	2.512650	1.584352
C	-3.439052	-3.398795	-2.393712	H	-0.434395	-2.839092	-0.091401
C	-3.498644	4.589413	0.534255	H	-5.437657	0.658921	0.018457
C	-2.679210	-4.509236	-2.019599	H	-5.475010	-1.000639	-0.521932
C	-2.399852	4.161188	1.283063	H	-6.074290	-1.161415	2.065437
C	-1.575877	-4.330278	-1.182097	H	-5.033835	-1.823525	4.225095
C	-1.871279	2.899032	1.032458	H	-2.546311	-1.670930	4.471840
C	-1.270552	-3.046827	-0.739711	H	-1.203178	-0.855282	2.500201
N	-2.006908	-1.975213	-1.106126	H	2.552529	2.057599	2.961154
N	-2.383296	2.082971	0.084832	H	1.020219	1.407910	2.354021
C	-4.805524	-0.213356	-0.165500	H	2.806196	-0.754090	3.481493
C	-4.191890	-0.647265	1.153261	H	1.222404	-0.715942	2.684360
C	-5.003179	-1.100865	2.199304	H	2.417548	4.424428	2.093090
C	-4.419498	-1.472206	3.408629	H	3.248946	-3.246236	3.491499
C	-3.030109	-1.387680	3.549207	H	2.180891	5.927315	0.117268
C	-2.279000	-0.935135	2.472607	H	3.602666	-5.308799	2.137650
N	-2.850032	-0.568395	1.298425	H	1.633979	4.932518	-2.110985
N	2.679233	0.362429	1.643291	H	3.139414	-5.248464	-0.319031
C	2.048153	1.647038	2.082042	H	1.383253	2.436398	-2.280318
C	2.295758	-0.795499	2.515473	H	2.323024	-3.093023	-1.332663
C	2.025053	2.644854	0.946570	H	4.494462	1.441968	1.934865
C	2.583690	-2.094159	1.798904	H	4.649337	-0.289563	2.109144
C	2.187517	4.018497	1.118019	H	6.731466	0.778575	0.530732
C	3.043922	-3.248738	2.430406	H	7.451270	0.545621	-1.840394
C	2.051949	4.860055	0.008089	H	5.734764	0.013702	-3.584897
C	3.242445	-4.404677	1.668372	H	3.330699	-0.257488	-2.853546
C	1.751922	4.308084	-1.238526				
C	2.983796	-4.374882	0.295787				
C	1.617065	2.924856	-1.347689				
C	2.532451	-3.187852	-0.277885				
N	2.334852	-2.076297	0.464857				
N	1.761988	2.117593	-0.275770				
C	4.174556	0.488987	1.508519				
C	4.663288	0.381724	0.083749				
C	6.010856	0.550106	-0.241920				
C	6.412599	0.418897	-1.571207				
C	5.457111	0.122351	-2.547671				
C	4.130490	-0.030706	-2.165078				
N	3.746855	0.097929	-0.870490				
O	-1.183639	0.614894	-2.173953				
H	-4.941437	1.771541	-2.033932				

References

1. Anderson, P. W. In *Magnetism*; Rado, G. T.; Suhl, H., Eds.; Academic Press: New York, 1963; Vol. 1, p 25.

2. Goodenough, J. B. *Magnetism and the Chemical Bond*. John Wiley & Sons: New York, 1963.